IJST, Transactions of Civil and Environmental Engineering, Vol. 35, No. C1, pp 63-79
Printed in The Islamic Republic of Iran, 2011

THE INFLUENCE OF MORTAR HEAD JOINTS ON THE IN-PLANE AND OUT-OF-PLANE SEISMIC STRENGTH OF BRICK MASONRY WALLS*

M. R. MAHERI[1],** M. A. NAJAFGHOLIPOUR[1] AND A. R. RAJABI[2]

[1]Dept. of Civil Engineering, Shiraz University, Shiraz, I. R. of Iran
[2]Dept. of Civil Engineering, Sarvestan Branch, Islamic Azad University, Sarvestan, I. R. of Iran
Email: maheri@shirazu.ac.ir

Abstract– A sound assessment of the in-plane shear and out-of-plane bending capacities of the load-bearing walls is imperative when conducting seismic assessment or seismic design of masonry buildings. The bulk of work on the subject so far has assumed uniform construction with the brick units connected to each other by mortar bed joints as well as head joints. However, in many construction practices, either for architectural purposes or for speeding up the construction process, the head joints are omitted. This omission may have a profound effect on the response and the strength capacities of the wall. In this paper, the results of a number of tests carried out on half-scale brick wall panels, having different material properties, with head joints and without head joints, are presented. The walls are subjected to in-plane shear, as well as out-of-plane bending pushover loads to failure and their load-displacement curves are established. Representing numerical models for the in-plane shear case are also analyzed and results are compared with those of the experiments. It is found that, depending on the material properties and the modes of failure of the wall, the head joints contribute 35% to 50% to the in-plane shear capacity of the wall. The contribution of the head joints to the out-of-plane flexural strength of the wall is also found to be substantial.

Keywords– Masonry, brick walls, head joints, seismic strength, in-plane shear, pushover test

1. INTRODUCTION

The masonry shear walls are the main seismic load resisting elements in unreinfored masonry buildings. The in-plane shear resistance and the out-of-plane bending capacity of the walls are their main lines of defense against earthquake loads. The shear and bending capacities of brick walls are, on the other hand, dependant on the ability of the horizontal mortar joints (bed joints) and the vertical mortar joints (head joints) to transfer the loads through the brick units.

Many investigators have studied the behaviour of masonry walls numerically or experimentally. One of the earliest works attributed to the first group was carried out by Johnson and Thompson [1]. In an experimental work, they presented a diametrical testing procedure for determining the in-plane shear resistance of brick masonry. They showed that if the load was applied in a direction at a 45° angle to the bed joint, the stresses in the wall and the subsequent failure of the wall will be in diagonal tension (shear). A similar work was conducted by Drysdale, et al. [2] on concrete block masonry with similar results. Based on the above findings Gabor et al. [3] investigated the shear behaviour of hollow-brick masonry panels by diagonally compressing them. The experimental results were used to propose efficient numerical modelling of the masonry. However, other investigators preferred to conduct in-plane shear tests on scaled

*Received by the editors January 28, 2009; Accepted August 15, 2010.
**Corresponding author

walls by applying the more realistic horizontal and vertical in-plane forces. The horizontal loading was applied in a variety of forms including pushover loading, cyclic loading and shake table loading. Manfredi and Mazzolani [4] conducted a review of different test methods and their applications and limitations.

One of the earliest tests on the scaled wall models undergoing horizontal and vertical in-plane loads was performed by Sinha and Hendry [5]. They concluded that the amount of pre-compression can affect both the mode of failure and the strength capacity of the wall and that, above a certain range of vertical compression, failure occurs in the diagonal tension, such that the crack passes through some of the brick units as well as through the mortar joints. The shear behaviour of brick masonry walls was also studied by Magenes and Calvi [6]. They looked at the main seismic response parameters of strength, deformability and energy dissipation capacity of brick walls. Also, in an experimental investigation, Tasnimi [7] compared the cyclic in-plane response of different types of reinforced and unreinforced masonry walls commonly constructed in Iran or recommended by Iranian seismic code. He concluded that using reinforced or confining the walls in concrete tie beams and column greatly increase the strength and ductility of the masonry wall. In a recent study, Kaltakci et al. [8] carried out cyclic tests on infill brick walls. They concluded that the ratio of the infill wall span/height considerably affects the lateral load bearing capacity and the energy dissipation capacity of the frame. They also showed that plastering of the wall, usually considered as a non-structural component, also considerably increases the strength and stiffness of the infill.

Following a number of major earthquakes in recent years in Iran and the general poor behaviour of the local brick masonry buildings, a number of investigators have looked at the seismic behaviour of brick masonry walls with varying qualities of local materials and workmanship. Razani and Lee [9] reported on the observed modes of failure of masonry walls and piers during the Qir earthquake of 1972. Maheri et al. also reported on the response of masonry buildings to the Manjil earthquake of 1990 [10] and the Bam earthquake of 2003 [11]. The above observations showed the diagonal and horizontal brick-mortar bond slippage to be the dominant mode of failure in brick shear walls. This was attributed to weak bond strength due to poor workmanship. Moghadam [12] carried out experimental investigations as well as theoretical evaluations to derive the response of local brick walls to in-plane shear.

Page [13], Lourenco and Rots [14], Giordano et al. [15], Kappos et al. [16] and many other investigators have also numerically studied the behaviour of masonry shear walls and have presented numerical models for analyzing this element.

A number of investigators have studied the behaviour of mortar bed joints and head joints and their effects on the global strength and response of the wall. The prevalent view of the behaviour of the mortar joint models the response on a Mohr-Columb shear failure mechanism, assigning bond strength and friction for bed joints. In an earlier study, Stafford-Smith and Carter [17] questioned this model and proposed that the failure of mortar bed joints occurs in tension, and therefore it may be predicted more rationally by comparing the actual tensile stresses in the mortar layer with its tensile strength. El-Sakhawy et al. [18] also investigated the behaviour of mortar joints in masonry walls under shear. They conducted some tests on the brick mortar bed joints to verify the modified elasto-plastic joint model of Fishman and Desai [19], and it was concluded that the modified elasto-plastic model predicts the shearing stress-displacement response reasonably well, although the prediction of the normal displacement field is not as good. Abdou et al. [20] investigated, experimentally, the brick-mortar bond behaviour.

On the effects of the head joints on the strength and response of the masonry wall, very little is reported. Mojsilovic and Marti [21] used a sandwich model to predict the strength of masonry wall elements subjected to combined in-plane forces and moments. In their model the head joints only contributed to transferring the compressive stresses and no transfer of shear was assumed between the

mortar bed joints and head joints. In another study, Schlegel and Rautenstrauch [22] numerically evaluated the effects of the head joints on the failure pattern of stone masonry. In their opinion, due to shrinkage of the head joints and the subsequent loss of bond between the stone and mortar, their contribution to the shear transfer is far less than that of the bed joints. In one of the numerical models, they assumed no bed joints and obtained a different failure pattern to that of the model with full head joints. However, they did not elaborate on the effects of the head joints on the shear strength of the stone wall. Considering the importance of being able to assess the real strength of brick walls constructed without head joints and the absence of sound information on the subject, in this paper, the effects of head joints on the in-plane shear and out-of-plane bending capacities of brick walls and their respective modes of failure are investigated experimentally. Numerical models are also analyzed for the in-plane shear case and the results are compared with those of the experiments.

2. IN-PLANE SHEAR INVESTIGATIONS

a) Experimental investigations

Test specimens and setup: In total, four single-layer brick wall panels were constructed for the in-plane shear experiments. The wall panels for these tests were 160cm wide, 140cm high and 11cm thick. Of the four panels, two were made with 'standard' materials and workmanship and two panels were constructed using 'non-standard' materials and workmanship. Also, in each pair of the standard and non-standard panels, one panel was constructed with mortar head joints and another without mortar head joints. The term; 'standard material' refers to brick units and mortar mixes compliant with internationally accepted norms for masonry construction. In constructing the standard walls, compressed pavement brick units were used. Also, the mortar was made of ordinary Portland cement and fine sand (passing sieve # 20) with a weight ratio of 1:3. Also, the term 'standard workmanship', refers to the use of the bricks in a state of saturated-surface dry, so that they do not drain the moisture of the mortar, and curing the wall panels under polythene sheet for 28 days against loss of moisture. So the brick-mortar bond was considerable in these samples. A number of samples were also made for the material and prism tests. These included; compressive and tensile tests on mortar, compressive and flexural tests on brick units, shear, compression and bending capacity tests of brickwork and determination of modulus of elasticity of mortar, brick units and brickwork. Results of the material and prism standard tests carried out according to the related ASTM standards are listed in Table 1.

Table 1. Material test results for the standard and non-standard brick panels

Property	ASTM standard	Standard walls	Non-standard walls
Comp. strength of brick unit (MPa)	C67-98a	11	13.8
Tensile (flexural) strength of brick unit (MPa)	C580-02	1.1	-
Comp. Strength of mortar (MPa)	C579-96, C39-99	34	6.6
Tensile strength of mortar (MPa)	C307-94, C496-96	4.4	.65
Young's modulus brick unit (MPa)		7500	-
Young's modulus mortar (MPa)	C580-02	12000	-
Young's modulus of brickwork (with head joint) (MPa)	C1314	-	7000
Young's modulus of brickwork (without head joint) (MPa)	C1314	-	1500
Shear bond Strength (MPa)	C1513	.0915	.005
Friction coefficient for brick mortar interface in headjoint	-	-	.85
Friction coefficient for brick mortar interface in bedjoint	-	-	1.2

The 'non-standard' wall panels were constructed with commonly used, non-engineered bricks and cement mortar. The traditionally fired bricks in Iran are generally weaker. Also, in making the cement mortar, instead of sand, fine aggregate is invariably used. In constructing the non-standard wall panels, a weight ratio of 1:4 was used for cement and fine aggregate (passing sieve # 4). Also, in accordance with common practice, in constructing the non-standard wall panels, the bricks were used in a dry state and no curing was performed on the constructed panels. So the brick-mortar bond was very weak in these panels.

The test set-up used in this study (Fig. 1) conforms to one of a number of test set-ups presented by Mayes and Clough [23-24] in their state of the art reports regarding the in-plane shear tests on masonry walls. In this set-up, two hydraulic jacks, one placed horizontally and the other vertically at the loading end of the concrete beam which was constructed on the wall, simultaneously exert equal loads on that corner of the wall. The loading step in all four tests was set at 3.0 kN. This loading step corresponded to 2% of the estimated ultimate capacity of the strongest panel. Four mechanical dial gauges were used to record the displacements of the wall specimens in each loading step. The positions of these gauges are also shown in Fig. 1.

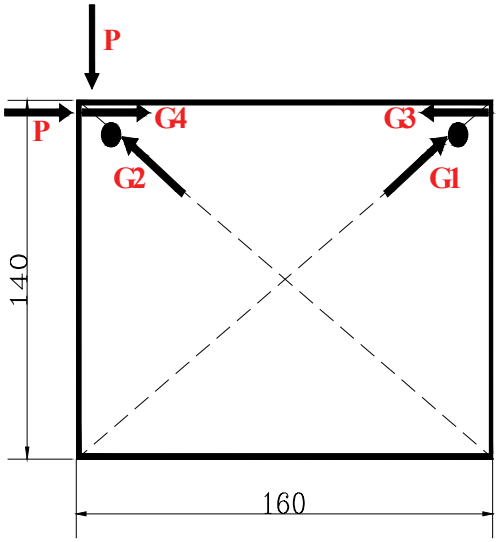

Fig. 1. Test setup for the in-plane shear loading of wall panels

Test of standard wall with head joints (SWFS): Considering the material properties and method of construction, the ultimate shear capacity of this wall was estimated as 150kN. The force-displacement pushover curve obtained for the drift (G_3) is plotted in Fig. 2. The force-displacement curve shown in Fig. 2 indicates a near linear response of the wall panel up to the 121 kN. A slight change in the slope of the curve beyond this load may correspond to the first cracking of the wall. However, during the test, no cracks became visible until the load of 140kN, at which the sudden and explosive failure of the wall panel occurred on the compression diagonal, (Fig. 3). The diagonal failure was primarily in the form of tensile failure of brick units and mortar joints with a major line crack and a number of smaller parallel cracks running through both materials. As it was expected, the brick-mortar bond slippage on the diagonal main crack was minimal. The drift measured at the load 121 kN is 0.83mm, giving a stiffness of 142 kN/mm.

Test of standard wall without head joints (SWES): The incremental pushover curve for drift measured for this wall during the in-plane shear test is plotted in Fig. 3. Similar to the response of the wall with head joints, an almost linear force-drift relation can be observed for this wall. The slope of the curve, however, changes markedly beyond 74 kN load, indicating some form of yielding of the wall panel. However, no cracking could be seen at this load. At 91.5 kN load, the failure of the wall occurred somewhat similar to that of the wall SWFS, with a sudden and explosive cracking on the compression diagonal (Fig. 4). The

main form of failure was, however, parallel diagonal tensile cracks through the bricks and mortar joints with very small sections of bond slippage.

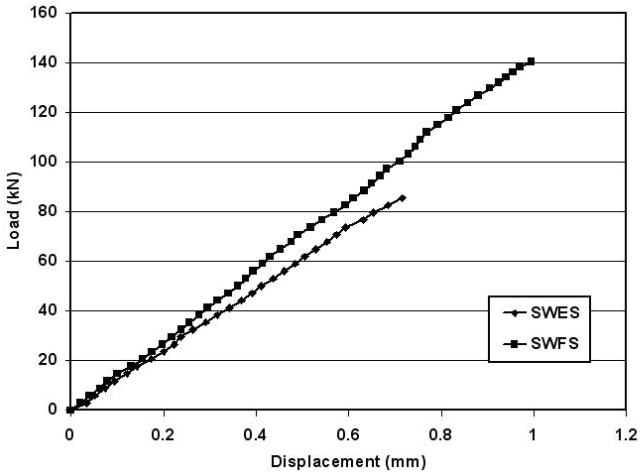

Fig. 2. Pushover curves of the walls SWFS and SWES

Fig. 3. Mode of failure of the wall SWFS

Fig. 4. Mode of failure of the wall SWES

The slope of the drift pushover curve, up to 74 kN provides a stiffness of 121 kN/mm for this wall. This stiffness is 15% less than the stiffness measured for the wall SWFS, indicating the stiffening effects of the head joints. By comparing the ultimate loads measured for the two walls, it becomes evident that the head joints had a 35% contribution to the in-plane shear capacity of the wall SWFS.

Test of non-standard wall with head joints (NWFS): The force-displacement curves for the non-standard wall with head joints (NWFS) are plotted in Fig. 5. The ultimate failure of the wall, at 31 kN load, was sudden. However, contrary to the failure of the standard walls it was not explosive. The main crack followed, more or less, the compression diagonal in a combination of horizontal and stepwise bond slippage (Fig. 6). The stiffness of this wall is calculated as 99 kN/mm.

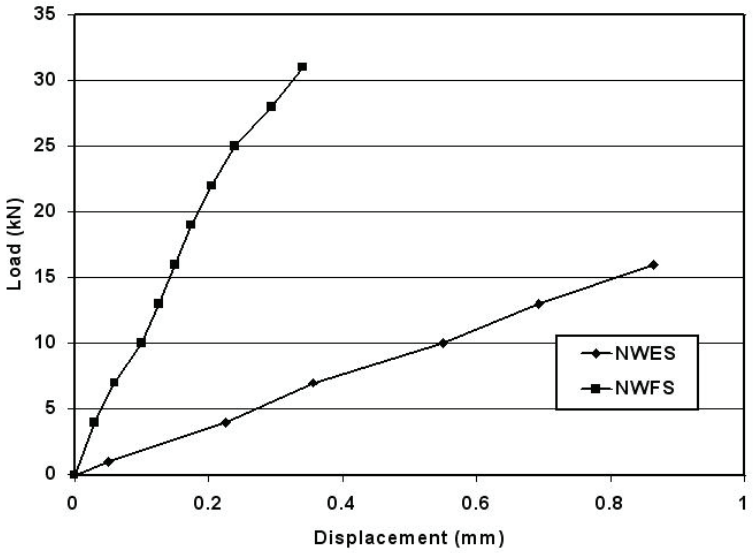

Fig. 5. Pushover curves of the walls NWFS and NWES

Fig. 6. Mode of failure of the wall NWFS

Test of non-standard wall without head joints (NWES): The pushover force-displacement curve deduced from the test of this wall is shown in Fig. 5. The main crack in the form of a classic and clean stepwise bond failure on the compression diagonal appeared at the load of 16 kN (Fig. 7). With the application of further loads, a somewhat ductile failure continued with widening of the stepwise crack.

The shear stiffness of this wall is calculated as 18.5 kN/mm. This is many folds less than the stiffness of the wall NWFS, indicating a drastic reduction in the stiffness of the wall due to the lack of head joints. By comparing the ultimate shear capacity of this wall with wall NWFS, the shear strength contribution of the head joints for these non-standard wall panels is measured as 48%, which is appreciably more than that for the standard walls. The results of the tests are summarized in Table 2.

Table 2. Results of the in-plane shear tests

Panel	Ultimate capacity (kN)	Stiffness (kN/mm)	Capacity reduction	Stiffness reduction
SWFS	140	142	35%	15%
SWES	91.5	121		
NWFS	31	99	48%	81%
NWES	16	18.5		

Fig. 7. Mode of failure of the wall NWES

a) Numerical investigations

Many different methods of analysis are available for URM. These range from such approximate methods as the equivalent frame method [16, 25] and the strut-tie method [26] to the more rigorous nonlinear FE analysis methods using macro [27] and micro models [28], as well as the distinct element method [29]. To achieve better accuracy, the micro model was adopted for numerical analyses of the standard walls and a simplified micro model was used for the non-standard walls. ANSYS, general-purpose program [30] was utilised to develop the numerical models and carry out the nonlinear pushover analysis of the wall panels

Numerical analysis of sndard wall panels: The element selected to model the brick units and mortar joints for the standard walls is the three-dimensional SOLID65. The material model adopted to represent the brick units and mortar is the 'concrete' model of ANSYS. The concrete material model in this program predicts the failure of brittle materials including masonry units. Both cracking and crushing failure modes are accounted for in the model. In the concrete material model, the criterion for failure of the brittle material due to a multi-axial stress state is of the form; $F/f_c - S > 0$ [31] where, F is a function of principal stresses expressed in four different failure domains, S is the failure surface, also expressed in terms of principal stresses and five input parameters including; the ultimate uniaxial compressive (f_c) and tensile (f_t) strengths, ultimate biaxial compressive strength (f_{cb}) and the ultimate compressive strength for a state of biaxial (f_1) and uniaxial (f_2) compression superimposed on hydrostatic stress s_h, itself being the average of

the three principal stresses. However, one needs to specify only the two constants, f_c and f_t. The other three constants may default to values given by Willam and Warnke [31]. Other input parameters for material include; the elastic modulus, Poisson's ratio (assumed 0.15 for both brick and mortar) and the shear strength reduction factor for open and closed crack states, assumed as 0.50 and 0.90, respectively.

In forming the micro models for the standard walls, it was deemed unnecessary to use interface elements to represent the bond strength between bricks and mortar. This was because the experimental results suggested that due to the type of mortar used in, and the moisture curing of, the standard walls, the strength of the bond between brick units and mortar was sufficient not to warrant modelling the interface. A very fine mesh was used for the micro model of the standard wall with head joints (SWFS). The mesh is shown in Fig. 8a.

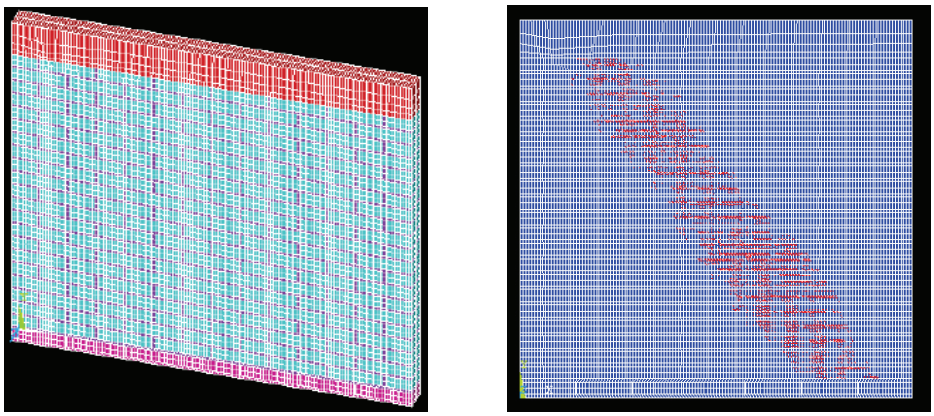

(a) (b)

Fig. 8. Standard wall SWFS, (a) The FE mesh of the micro model, (b) ultimate crack pattern

The pushover curve, representing the relation between the incremental load and the corresponding in-plane drift for this wall is plotted next to the experimental curve in Fig. 9a. Close agreements could be seen between the two curves, numerical shear strength being around 9% less than the experimental capacity at a similarly reduced drift level. It shows a linear response of the wall up to the load 120kN. No cracking was seen in the results for this range. Beyond this load, the first cracks develop in the vicinity of the compression diagonal and rapidly spread to cover the entire compression diagonal zone (Fig. 8b). The spreading of the cracks can be deduced from the force-drift curve of Fig. 9a in the form of the change of the slope at the end of the curve. The shear stress distribution in the wall at the ultimate load corresponds well with both the numerical cracking zone and the experimental cracking pattern.

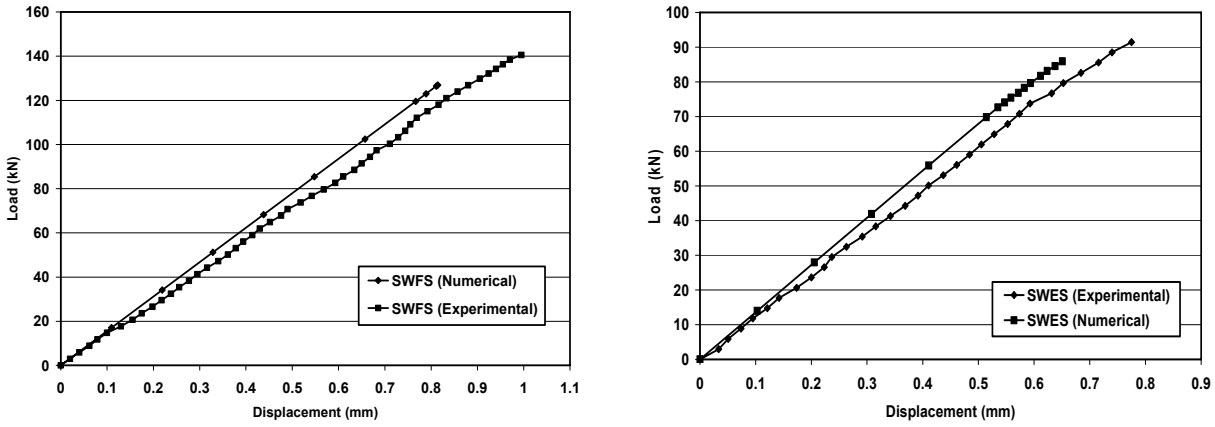

(a) (b)

Fig. 9. Comparison between the pushover curves of the standard wall panels; (a) with head joints (SWFS) and (b) without head joints (SWES)

The nonlinear pushover analysis of the standard wall panel, SWES, was performed in a similar manner to the wall SWFS. The numerical pushover curve for this wall is plotted next to the experimental curve in Fig. 9b. Similar to the experimental response curve, the numerical curve shows a marked, albeit short, ductile zone. This indicates the dominance of the mortar bed joints in forming the response of the brickwork at failure. Formation of cracks could be seen to be different to that of the wall with head joints (SWFS). However, similar to wall SWFS, the numerical shear strength evaluated for this wall is also less than the experimental value, the difference being around 6%.

Numerical analysis of non-standard wall panels: A simplified micro model was developed to conduct nonlinear pushover analysis of the non-standard wall panels. This is because, unlike the standard walls, the response and the failure mode of the non-standard walls are dictated by the brick-mortar bond strength. To model the non-standard walls, therefore, a relatively fine micro model with interface elements was used. In this model, brick units together with half of their surrounding mortar are represented by a number of elements having identical material properties. Interface elements were used to join the brick-mortar elements at the middle of the mortar joints. The response of these elements is governed by Mohr-Columb criterion. The properties assumed for the elements, including the shear bond strength and friction coefficient, were deduced from the material tests (Table 1). The simplified micro model thus formed for the wall NWFS is shown in Fig. 10a. It should be noted that the equivalent brick-mortar elements are assumed to have linear responses. Considering the dominance of the bond strength, represented by the interface elements, on the shear response of these non-standard walls, such an approximation should not influence the results.

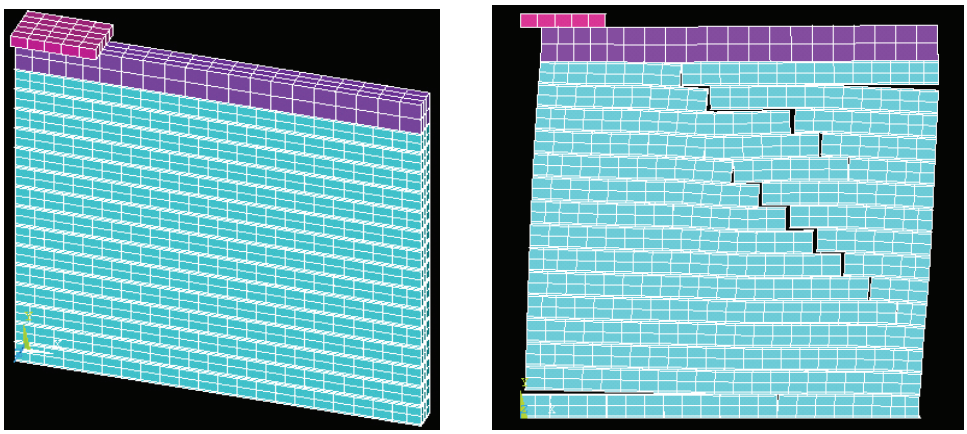

(a) (b)

Fig. 10. Non-standard wall NWFS, (a) The FE mesh of the micro model, (b) ultimate crack pattern

The pushover curve evaluated for the wall NWFS using this numerical model is shown, superimposed on the experimental pushover curve for the same wall in Fig. 11a. The numerical curve follows a similar trend to the experimental curve up to a load of 25 kN, where the analysis stops as the ultimate wall capacity. This is 20% less than the experimental capacity. The relatively large discrepancy can be attributed to the variations in the material properties of the wall panel and the properties used for the numerical models obtained from material tests. The failure pattern for this wall, shown in Fig. 10.b, however, closely resembles the experimental failure pattern with initial horizontal cracking one brick layer below the concrete beam followed by the diagonal and horizontal bond slippage.

Similar behaviour could be seen when comparing the numerical pushover curve for the non-standard wall without the head joints with that obtained in the experiment (Fig. 11b). The numerical curve shows a stiffer response, giving an ultimate capacity of 12.6 kN, 11% less than the experimental capacity.

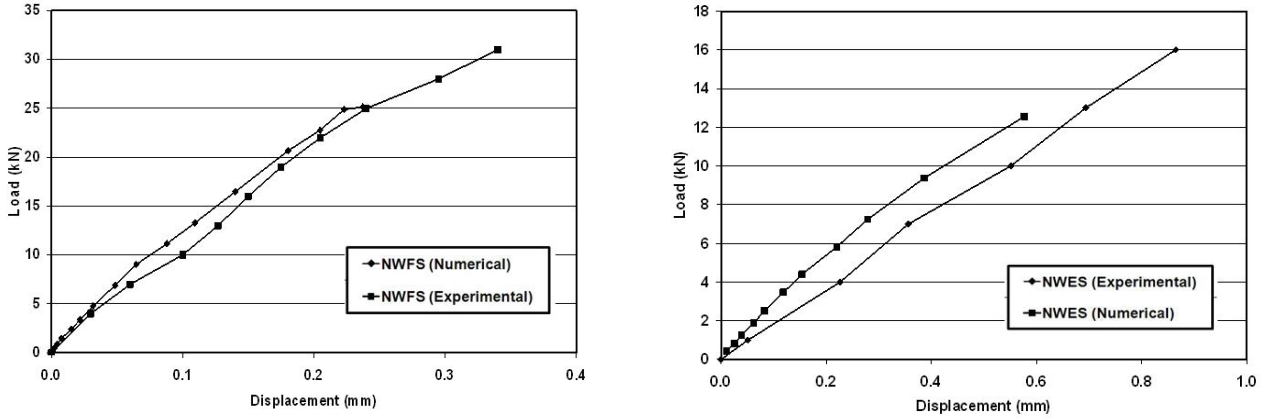

(a) (b)

Fig. 11. Comparison between the pushover curves of the non-standard wall panels; (a) with head joints (NWFS) and (b) without head joints (NWES)

When the results of the standard walls are compared with those of the non-standard walls, a sharp decline in the latter is observed, the standard wall without head joints being over five folds stronger than its non-standard counterpart, and the standard wall with head joint being 4.5 times stronger than its corresponding non-standard wall. These disproportionate differences are caused primarily by poor workmanship in the form of using dry brick units and not water curing the wall after construction; a fact easily noted when we compare the strength properties of the standard and non-standard mortars.

3. OUT-OF-PLANE FLEXURAL INVESTIGATIONS

a) Test specimens and setups

Similar to the in-plane shear investigations, four single-layer brick wall panels were constructed for the out-of-plane bending experiments. The wall panels for these tests were 120cm square. Of the four panels, two were made with standard materials and workmanship and two were constructed using non-standard materials and workmanship. Also, in each pair of the standard and non-standard panels, one panel was constructed with mortar head joints and another without the mortar head joints. The test set-up for the out-of-plane testing of the wall panels is shown in Fig. 12a. It consists of a loading frame, against which a horizontally placed hydraulic jack exerts the out-of-plane point load on the specimens. Five mechanical dial gauges were used to record the deflections of each specimen. The locations of these gauges are shown in Fig. 12b.

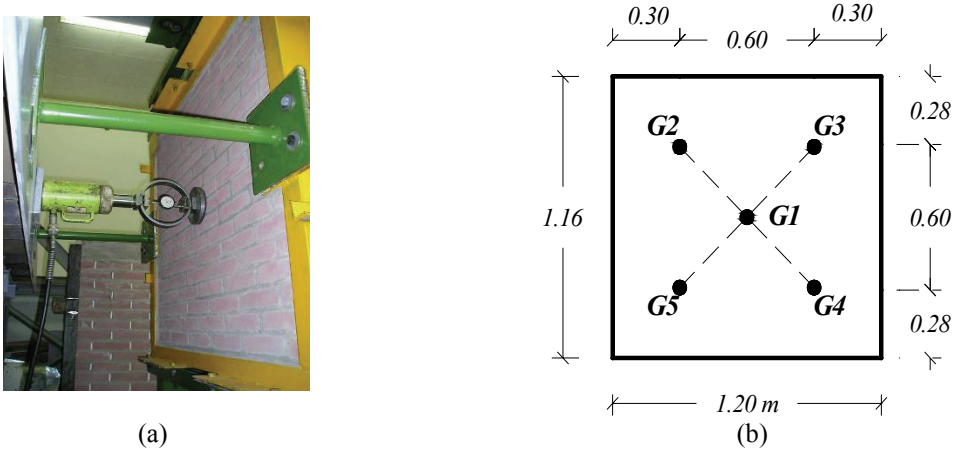

(a) (b)

Fig. 12. (a)Test setup (b) position of mechanical gauges in the out-of-plane bending tests

b) Test of standard wall with head joints (SWFB)

The out-of-plane incremental loading of the standard wall panels with head joints (SWFB) and without head joints (SWEB) was carried out in 0.25 kN steps and in each step, the corresponding displacements were recorded. The force-controlled pushover curves thus obtained for the test panel SWFB are plotted in Fig. 13. This figure indicates that the response of the panel with the head joints is linear throughout the panel up to a load of 14 kN; the linear stiffness being about 88.3 kN/mm using the displacements for the centre of the panel, (Fig. 13).

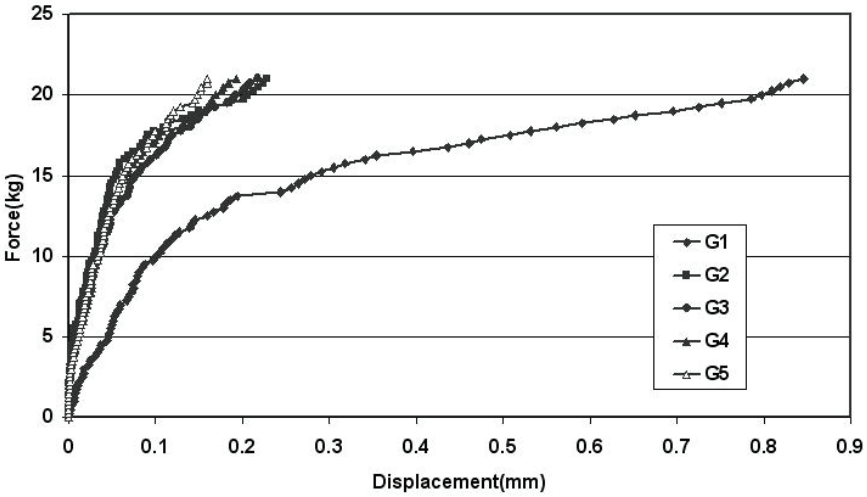

Fig. 13. Pushover curves of the wall SWFB

Figure 13 also indicates that the first crack occurred at the same load of 14 kN. The crack, however, did not become visible until the load reached the value of 17 kN. Contrary to the yield line theory prediction for isotropic materials, the first crack occurred almost vertically at the centre of the panel (Fig. 14). The formation of this crack reinforced the notion that the masonry wall is stiffness orthotropic. Following the reduction in the stiffness of the panel in the horizontal direction and the redistribution of stresses, the panel started to behave increasingly isotropic. The change from the orthotropic behaviour to isotropic performance was noted when at the ultimate load of 21 kN, simultaneous diagonal cracking, pertinent to an isotropic behaviour occurred (Fig. 14).

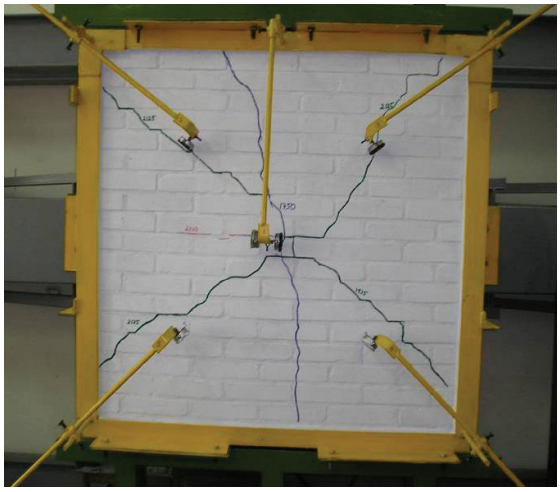

Fig. 14. Mode of failure of the wall SWFB

c) Test of standard wall without head joints (SWEB)

The pushover curves obtained for the SWEB panel are plotted in Fig. 15. The data for all five locations show that the first major change of slope occurred at 9.5 kN. The crack itself became visual at the load 10.7 kN in the form of a vertical crack running along the centre of the panel (Fig. 16). This crack was similar in position and orientation to the first crack that occurred in the sample SWFB. It did, however, occur at a load 32% less than the corresponding load in the sample SWFB. This indicates a considerable decrease in the out-of-plane capacity of the panel due to the omission of the head joints.

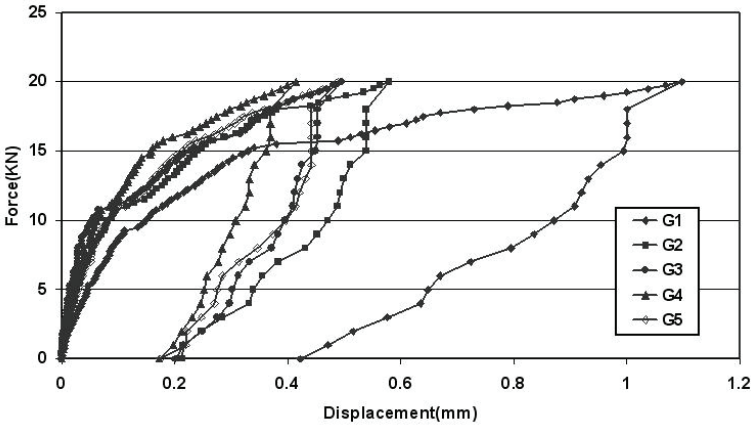

Fig. 15. Pushover curves of the wall SWEB

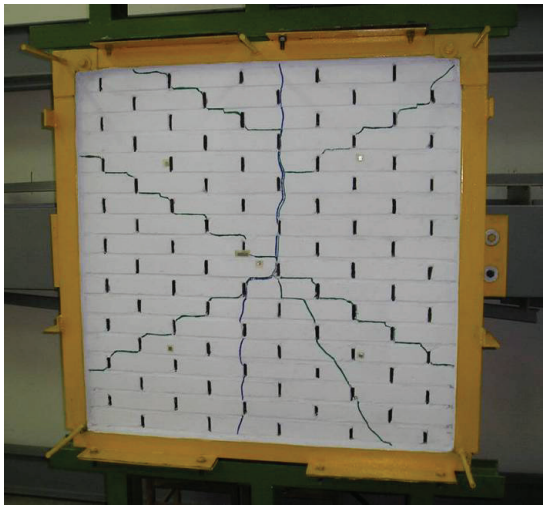

Fig. 16. Mode of failure of the wall SWEB

The occurrence of the vertical crack indicates that this panel also behaved initially orthotropic. The linear stiffness was about 82.6 kN/mm using the displacements for the centre of the panel. The force-deflection curves indicate a further softening of the panel at 15.5 kN. This softening became visible during the test at a load of 15.75 kN by the formation of a cross-diagonal crack (Fig. 16), similar to that which occurred in the panel SWFB at the higher load of 21 kN. Contrary to the behaviour of panel SWFB, which could not sustain further load beyond that point, the panel SWEB continued to carry further loads at higher deflections, indicating a substantial ductile performance. The load was increased to 20 kN, at which load was due to excess opening of the cracks. It was decided to discontinue loading up and to unload to obtain a complete half cycle (Fig. 15). Noting that the test procedure adopted here was force-controlled as opposed to displacement-controlled, the results of the post-peak unloading of the panel seen in Fig. 15

may not be an accurate representation of the behavior of the panel during the unloading branch. They are, however, presented to gain an insight into the effects of the different conditions on the ductility response.

d) Test of non-standard wall with head joints (NWFB)

The out-of-plane loading of the non-standard wall panel with head joints (NWFB) was carried out at 0.25kN loading steps and at each step the wall displacements at the five locations shown in Fig. 8b were recorded. The load-displacement pushover curves for the five positions recorded are plotted in Fig. 17. Observations made during the test showed that the first cracks appeared in the wall at around 2.5 kN. These cracks were diagonal, following more or less the pattern indicated by the yield line theory of isotropic materials. The cracks also appeared exclusively on the joints between the bricks and mortar. This indicates the weak bond between the two materials. The cracks at 2.5 kN can also be deduced from the pushover curves of Fig. 17, at which the load change of the slope can be seen for all locations recorded. After that, a gradual decrease in the slope of the curves can be seen as the diagonal crack spread to cover the entire panel and a second set of diagonal cracks developed. Also, in line with an expected orthotropic response, a vertical line along the brick-mortar joints (Fig. 18) also appeared. The non-linear, somewhat ductile response of the panel continued, as the load increased to 12 kN. At this load, due to widening of the cracks it was decided to unload the frame and record the response to unloading.

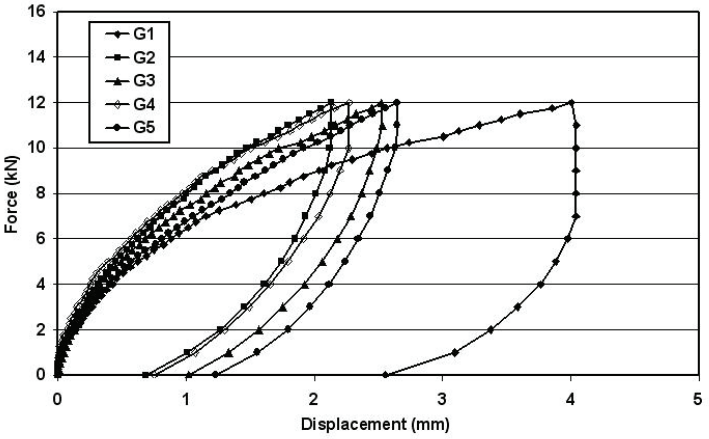

Fig. 17. Pushover curves of the wall NWFB

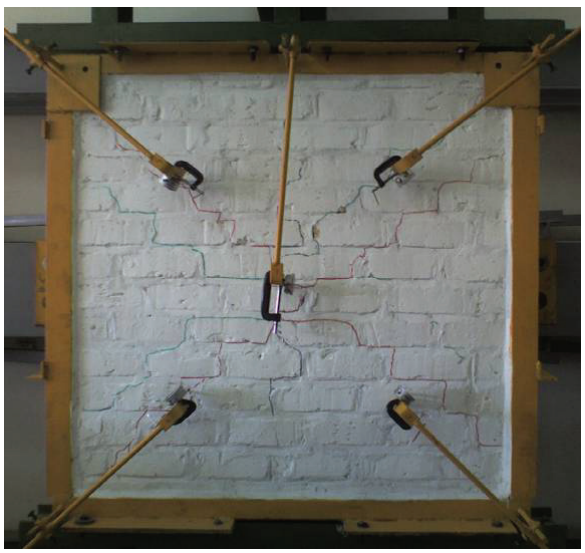

Fig. 18. Mode of failure of the wall NWFB

e) Test of non-standard wall without head joints (NWEB)

The out-of-plane loading of the non-standard wall panel without head joints (NWEB) was carried out in a similar manner to the previous tests. Figure 19 shows the force-displacement pushover curves for the five locations measured during the test. The loading was continued to the same level as the wall NWFB (12 kN), after which unloading was performed. The first softening of the wall appears to have occurred at the load of 1.75 kN. A second marked change of slope can be seen around 4.0 kN load, after which a gradual softening of the panel can be deduced from all five recording gauges. The failure pattern of this infill wall before unloading is shown in Fig. 20. By comparing the results of walls NWFB and NWEB, a marked decrease in the overall stiffness due to the omission of head joints can be seen. The test results are summarized in Table 3.

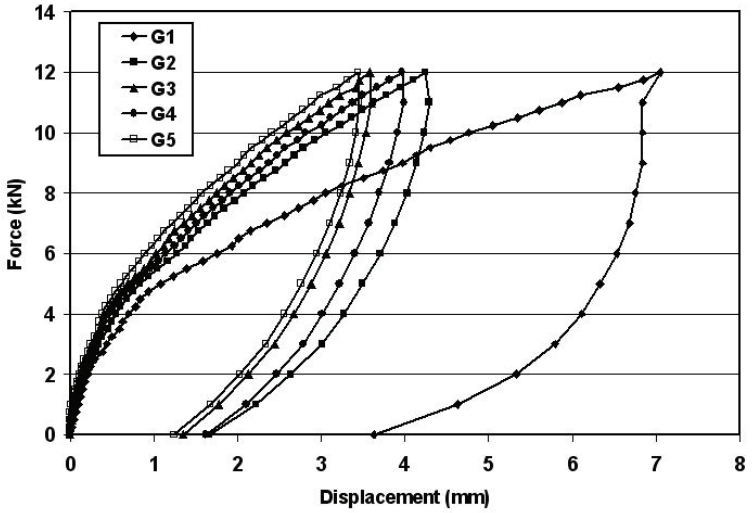

Fig. 19. Pushover curves of the wall NWEB

Fig. 20. Mode of failure of the wall NWEB

Table 3. Results of out of plane tests

Panel	First crack (kN)	Second Crack (kN)	Stiffness (kN/mm)	First crack capacity reduction	Second crack capacity reduction	Stiffness reduction
SWFB	14	21	88.3	32%	26%	7%
SWEB	9.5	15.5	82.6			
NWFB	2.5	5.25	16.4	30%	23%	48%
NWEB	1.75	4	8.6			

4. CONCLUSION

The earthquake capacity of masonry walls are shown to be adversely affected by the omission of mortar head joints. Results of in-plane shear and out-of-plane flexural tests of standard and non-standard brick masonry wall panels, aimed at determining the effects of the above parameter, lead us to draw the following conclusions:

1- The mortar head joints have a considerable effect on the in-plane shear capacity of brick walls. For the walls having different materials and different behaviour (i.e standard walls with high brick-mortar bond strength and non-standard walls with weak brick-mortar bond), lack of head joints resulted in reductions of 35% to 48%.

2- In both panels of standard walls, because of the high brick-mortar bond strength, the brick-mortar bond slippage on the diagonal main crack was minimal. But in the non-standard wall panels, the diagonal crack appeared in a stepwise slippage form.

3- Omitting the head joints also substantially reduces the out-of-plane yield strength and stiffness of the walls. Reduction is around 30%. Post yield point, this omission has a reduced effect on the stiffness and the ultimate strength.

4- In walls without head joints, the bed joints dominate the response of the wall to out-of-plane bending. Lack of mortar in head joints causes a change in the performance of a wall subjected to biaxial bending from a relatively brittle response, to a largely ductile behaviour.

5- The influence of the lack of head joints on the in-plane shear and out-of-plane bending capacities of brick walls should be considered in the seismic vulnerability evaluation of such walls and appropriate retrofitting measures adopted. Injection procedure to fill the head joints may not be practical in many cases. Global retrofitting of the wall, such as shotcreting, may be more appropriate.

Acknowledgement- The authors wish to acknowledge the financial support provided for the work presented here by the Researchers' Support Fund of Iran under grant No. 84/3477.

REFERENCES

1. Johnson, F. B. & Thompson, J. N. (1969). *Development of diametral testing procedures to provide a measure of strength characteristics of masonry assemblages*. Designing, Engineering and Constructing with Masonry Products, Gulf Publishing Company, Houston, pp. 51-57.
2. Drysdale, R. G., Hamid, A. A. & Heidebrecht, A. C. (1979). Tensile strength of concrete masonry, *Journal of Structural Division, ASCE*, ST7, pp. 1261-1276.
3. Gabor, A., Ferrier, E., Jacquelin, E. & Hamelin, P. (2006). Analysis and modelling of in-plane shear behaviour of hollow brick masonry panels. *Construction and Building Materials*, Vol. 20, No. 5, pp. 308-321.

4. Manfredi, G. & Mazzolani, S. (1992). Review of existing in experimental testing of masonry structures subjected to horizontal loads, *Proceedings of the 10th World Conference on Earthquake Engineering*, Madrid, pp. 3557-3562.
5. Sinha, B. P. & Hendry, A. W. (1969). *Racking tests on storey-height shear wall structures with openings subjected to pre-compression*. Designing, Engineering and Constructing with Masonry Products, Gulf Publishing Company, Houston, pp. 192-199.
6. Magenes, G. & Calvi, G. M. (1997). In-Plane seismic response of brick masonry walls. *Earthquake Engineering and Structural Dynamics*, Vol. 26, pp. 1091-1112.
7. Tasnimi, A. (2004). *Performance of brick buildings in standard 2800*. Iran, Tehran: Housing and Building Research Centre of Iran, Publication No. G-404, (in Persian).
8. Kaltakci, M. Y., Koken, A. & Korkmaz, H. H. (2008). An experimental study on the behavior of infilled steel frames under reversed-cyclic loading. *Iranian Journal of Science and Technology, Transaction B: Engineering,* Vol. 32, No. B2, pp. 157-160.
9. Razani, R. & Lee, K. L. (1973). The engineering aspects of the Qir earthquake of April 10, 1972 in Southern Iran. *National Academy of Engineering*, Washington D.C.
10. Maheri, M. R. (1990). Engineering aspects of Manjil, Iran earthquake of June 1990. *A Field Report by EEFIT,* W.S. Atkins Engineering Sciences, Leatherhead, U.K., Publication No. G8630/90/001.
11. Maheri, M. R., Naeim, F. & Mehrain, M. (2005) Performance of adobe residential buildings in the 2003 Bam, Iran, earthquake, *Earthquake Spectra*, Vol. 21, No. S1.
12. Moghadam, H. (2001). Seismic design of brick buildings. *Sharif University Scientific Publications*. Tehran, Iran (in Persian).
13. Page, A. W. (1978). Finite element model for masonry. *Journal of the Structural Division, ASCE*, Vol. ST8, pp. 1267-1285.
14. Lourenco, B. P. & Rots, J. G. (1997), Multisurface interface model for analysis of masonry structures. *Journal of Structural Engineering, ASCE,* Vol. 123, No. 7, pp. 660-668.
15. Giordane, E., Mele, E. & De Luca, A. (2002), Modelling of historical masonry structures: comparison of different approaches through a case study. *Engineering Structures*, Vol. 24, pp. 1057-1069.
16. Kappos, A. J., Penelis, G. G. & Drakopoulos, C. G. (2002), Evaluation of simplified models for lateral load analysis of unreinforced masonry buildings. *J. Struct. Eng.*, Vol. 128, No. 7, pp. 890-897.
17. Stafford-Smith, B. & Carter, C. (1971). Hypothesis for shear failure of brickwork. *Journal of Structural Division, ASCE*, Vol. ST4, pp. 1055-1062.
18. El-Sakhawy, N. R., Raof, H. A. & Gouhar, A. (2002), Shearing behaviour of joints in load bearing masonry wall. *Journal of Materials in Civil Engineering*, Vol. 14, No. 2, pp. 145-150.
19. Fishman, K. L. & Desai, C. S. (1987), A constitutive model for hardening behaviour of rocj joints. *Constitutive Law for Engineering Materials: Theory and Application*, C.S. Desai et-al eds. Elsevier, New York, pp. 1043-1050.
20. Abdou, L., Saada, R. A., Meftah, F. & Mebarki, A. (2005), Experimental investigation of the brick-mortar interface behaviour. Experimental investigation of the mortar joint in masonry structures, *Mechanics Research Communications*, MRC 969.
21. Mojsilovic, N. & Marti, P. (1997). Strength of masonry subjected to combined actions. *ACI Structural Journal*, Vol. 94-S57, pp. 633-641.
22. Schlegel, R. & Rautenstrauch, K. (2004), Failure analysis of masonry shear walls. *Proceedings of the 1st Int. UDEC/3DEC Symposium on Numerical Modelling of Discrete Materials in Geotechnical Eng., Civil Eng. And Earth Science*, Bochum, Germany.
23. Mayes, R. L. & Clough, R. W. (1975). *A literature survey-compressive, tensile, bond and shear strength of masonry*. EERC 75-15, College of Engineering, University of California.

24. Mayes, R. L. & Clough, R. W. (1975). *State-of-the-art in seismic shear strength of masonry-an evaluation and review*. EERC 75-21, College of Engineering, University of California.
25. Magenes, G. & La Fontana, A. (1998). Simplified nonlinear seismic analysis of masonry buildings. *Proc. British Masonry Society*, No. 8, pp. 190-195.
26. Roca, P. (2006). Assessment of masonry shear-walls by simple equilibrium models. *Construction and Building Materials*, Vol. 20, No. 4, pp. 229-238.
27. Berto, L., Saetta, A., Scotta, R. & Vitaliani, R. (2004), Shear behaviour of masonry panel: parametric FE analyses. *Int. J. Solids and Structures*, Vol. 41, pp. 4383-4405.
28. Zucchini, A. & Lourenco, P. B. (2002). A micro-mechanical model for the homogenisation of masonry. *Int. J. Solids and Structures*, Vol. 39, pp. 3233-3255.
29. Giordane, E., Mele, E. & De Luca, A. (2002). Modelling of historical masonry structures: comparison of different approaches through a case study. *Engineering Structures*, Vol. 24, pp. 1057-1069.
30. ANSYS Inc. (2005). ANSYS user's manual, revision 9, SAS IP, Houston.
31. Willam, K. J. & Warnke, E. P. (1975) Constitutive models for the triaxial behaviour of concrete. *Proc. Int. Assoc. Bridge Struct. Eng. Sem. Concr. Struct. Subjected Triaxial Stresses*, Vol. 19, pp. 1-30, Bergamo, Italy.